

Comparison of Real-time Three-dimensional Gadolinium-enhanced Elliptic Centric-ordered MR Venography and Two-dimensional Time-of-flight MR Venography of the Intracranial Venous System

Jui-Hsun Fu, Ping-Hong Lai*, Chia-Chi Hsiao, Shang-Chieh Li, Mei-Jui Weng, Po-Ching Wang,
Clement Kuen-Huang Chen

*Department of Radiology, Kaohsiung Veterans General Hospital, Kaohsiung, and National Yang-Ming
University School of Medicine, Taipei, Taiwan, R.O.C.*

Background: To compare 3-dimensional gadolinium-enhanced elliptic centric-ordered (3D GEC) magnetic resonance venography (MRV) with traditional 2-dimensional time-of-flight (2D TOF) MRV for imaging of the intracranial venous system. **Methods:** Fifty-three patients underwent 2D and 3D MRV, whereby venous structures were evaluated by 2 neuroradiologists. **Results:** Of the 53 patients, 10 were diagnosed with dural venous sinus thrombosis and 12 with intracranial tumors. 3D GEC MRV displayed superior sensitivity/specificity (90.9%/96.8%) compared to 2D TOF MRV (63.6%/48.4%). Analysis of the areas under the receiver operating characteristic curves also showed superiority of 3D GEC (0.91) versus 2D TOF (0.53) MRV. Of the remaining 31 healthy patients, the rate of complete visibility of venous structures was also greater for 3D GEC (95.8%) than for 2D TOF (62.1%) MRV. **Conclusion:** 3D GEC MRV is superior to 2D TOF MRV for providing more detail of the intracranial venous system, and can lead to better diagnosis of venous conditions. [*J Chin Med Assoc* 2010;73(3):131–138]

Key Words: intracranial venous system, magnetic resonance venography

Introduction

Imaging of the complex intracranial venous system is important in a variety of clinical situations, such as the diagnosis of intracranial venous thrombosis and the preoperative assessment of meningioma or other intracranial tumors, in which the patency of adjacent dural venous sinuses need to be clearly depicted. Conventional catheter angiography has traditionally been considered the standard of reference for imaging the intracranial venous system.¹ This is, however, an invasive procedure with well-known associated risks such as transient or permanent neurologic complications and puncture-site hematomas.²

Two-dimensional time-of-flight (2D TOF) magnetic resonance venography (MRV) has been widely used as a noninvasive means of visualizing the intracranial

venous system.^{3,4} However, a major limitation of 2D TOF MRV is the artifactual intravascular signal loss either due to in-plane saturation of spins or tortuosity and turbulent flow that occurs at certain points, namely, the posterior portion of the superior sagittal sinus, torcular herophili, transverse sinus, transverse-sigmoid junction, and sigmoid sinuses.^{5,6} To overcome this limitation, contrast-enhanced MRV techniques have been proposed, such as 3-dimensional gadolinium-enhanced elliptic centric-ordered (3D GEC) MRV.⁶ 3D GEC MRV is flow-insensitive, and common flow-related artifacts seen on 2D TOF MRV can be avoided. The repetition time is shortened, the signal of background tissue is suppressed to a greater degree, and images of higher spatial resolution are obtained in less scanning time with 3D GEC MRV than with 2D TOF MRV.^{6,7} However, there are few reports in the literature of 3D



*Correspondence to: Dr Ping-Hong Lai, Department of Radiology, Kaohsiung Veterans General Hospital, 386, Ta-Chung 1st Road, Kaohsiung 813, Taiwan, R.O.C.
E-mail: phlai@isca.vghks.gov.tw • Received: October 8, 2009 • Accepted: January 21, 2010

GEC MRV for imaging of the intracranial venous system.^{6,7} Farb et al⁶ published their initial experience in 2003, but they lacked systematic comparison of the imaging quality and diagnostic value of 3D GEC MRV with those of 2D TOF MRV.

The purpose of this study was to retrospectively evaluate the quality and investigate the diagnostic value of 3D GEC MRV for imaging the intracranial venous system versus conventional 2D TOF MRV techniques.

Methods

Patients

From July 2004 through February 2009 at Kaohsiung Veterans General Hospital, 3D GEC MRV and 2D TOF MRV were both performed in 53 patients (20 men, 33 women; age range, 16–76 years; mean age, 46.6 years).

All patients underwent MR examinations that included administration of contrast agent and imaging of the venous system. Examinations were requested by physicians for clinical reasons including possible dural sinus thrombosis and elucidation of venous anatomy in relation to a known intracranial tumor. Informed consent for administration of contrast material and MR examination was obtained from all patients. The final clinical diagnosis was based on the discharge report.

MR examinations

All examinations were performed using a superconducting 1.5-T MR system (Signa Excite HD; GE Medical Systems, Milwaukee, WI, USA) with a standard head coil.

The routine imaging studies included axial and coronal T1-weighted spin-echo [500/30/2 (repetition time/echo time/excitations)], T2-weighted fast spin-echo (4,000/100/2) with echo train length 8, fast fluid-attenuated inversion recovery [9,000/2,200/133/1 (repetition time/inversion time/echo time/number of excitations)] and diffusion-weighted imaging using a single-shot spin-echo echo-planar imaging [10,000/93 (repetition time/echo time)] with diffusion sensitivity $b=0$ s/mm² and $b=1,000$ s/mm². Axial, coronal, and sagittal postcontrast T1-weighted images were acquired.

2D TOF MRV with coronal acquisition from occiput to the coronal suture used the following parameters: 23/4.0 (repetition time msec/echo time msec); flip angle, 50°; fractional echo acquisition; field of view, 24 cm; matrix, 256 × 256; bandwidth, 15.6 kHz; section thickness, 2 mm; and acquisition of approximately 60–65 sections, yielding a total imaging time

of approximately 5 minutes. Resulting voxel dimensions were 0.96 × 0.96 × 2 mm.

In 3D GEC MRV, coordination of the intravenous injection of contrast medium and the start of imaging was performed using a software-based triggering tool (Fluoro Trigger). Details of this trigger method have previously been reported.⁸ Briefly, at the outset, a combined 2D fluoroscopic and 3D angiographic pulse sequence was loaded into the pulse sequence controller of the MR imager. The region of interest of the 2D fluoroscopic sequence was placed over the superior sagittal sinus. The MR technologist monitored the fluoroscopic scanning after contrast medium injection began, and the 3D angiographic pulse sequence was initiated immediately after sinus opacification was seen.

For contrast medium injection during MR imaging, a 2-cylinder MR-compatible injector (Optistar Mallinckrodt; Covidien Imaging Solutions, Hazelwood, MO, USA) was used. Intravenous access was obtained with a 22-gauge intravenous catheter located in the right antecubital vein. Twenty-five milliliters of contrast material was injected at a rate of 2–2.5 mL/sec and was followed immediately with a 30-mL bolus of normal saline at the same rate. This injection protocol was followed for all patients.

A 3D GEC fast spoiled gradient-echo sequence was oriented in the sagittal plane with coverage from ear to ear by using the following parameters: 5.8/1.9 (repetition time msec/echo time msec); flip angle, 35°; fractional echo acquisition; field of view (FOV), 25 cm; matrix, 320 × 320; phase FOV, 0.8; number of excitations, 0.75; bandwidth, 62.5 kHz; section thickness, 1.4 mm; 128 sections, resulting in a 17.9-cm-thick volume; and an imaging time of 2 minutes 28 seconds. Resulting voxel dimensions were 0.78 × 0.78 × 1.4 mm.

Post-imaging processing and reading

Source image data obtained with 2D TOF and 3D GEC MRV were transferred to a workstation (Advantage Windows, version 4.2; GE Medical Systems) for image manipulation. Maximum intensity projections were created for each TOF and GEC MRV data set, and rotated to provide 12 images (1 maximum intensity projection every 15° through 180° of rotation).

Two experienced neuroradiologists independently assessed the visibility of 15 predefined intracranial venous structures at each MRV examination: superior and inferior sagittal sinuses, straight sinus, right and left transverse and sigmoid sinuses, right and left junctions of the transverse and sigmoid sinuses, torcular herophili, vein of Galen, right and left basal veins of Rosenthal, and right and left internal cerebral veins. Visualization of these structures was reported as not visible, partially

visible, or completely visible. In addition, interobserver agreement was evaluated using κ statistics.

All conventional MR and MRV images were reviewed independently by the 2 readers, who were blind to the final diagnosis. The imaging diagnoses were made by consensus of the 2 readers. The sensitivity, specificity, positive predictive value and negative predictive value of the imaging diagnosis of each 2D TOF MRV and 3D GEC MRV with respect to a final diagnosis were calculated to assess the efficacy of these modalities. To compare the performance of these 2 imaging modalities, receiver operating characteristic (ROC) curve analysis was performed, and the 2 areas under the ROC curves (AUCs) were calculated and compared since they are measurements of the overall performance of the 2 different diagnostic tests.⁹ The software used for statistical analysis was STATA version 8.0 (Stata, College Station, TX, USA) for Windows. A *p* value less than 0.05 was considered to indicate a significant difference.

Results

Of the 53 patients examined, 10 were diagnosed with dural venous sinus thrombosis. In 5 of these cases,

2D TOF MRV could not differentiate thrombosis from dural sinus hypoplasia, resulting in a wrong imaging diagnosis (Figure 1). This therefore depicts the pitfalls of the 2D TOF MRV method. The extent of thrombosis was overestimated in 3 patients using 2D TOF MRV as compared with 3D GEC MRV (Figure 2). Two patients with chronic venous sinus thrombosis were initially missed by 3D GEC MRV, but were found by source image data and confirmed by conventional catheter angiography.

In addition, 12 of the 53 patients examined were diagnosed to have intracranial tumors. One patient had a metastatic tumor, while the other 11 displayed a meningioma. Six of these patients had a tumor without venous sinus invasion, whereby 3D GEC and 2D TOF MRV imaging were equivalent in the depiction of patent superior sagittal sinus. The other 6 patients displayed tumor with venous sinus invasion. 3D GEC and 2D TOF MRV were equivalent in the depiction of invaded dural sinuses in 3 patients, but 3D GEC MRV demonstrated residual blood flow in the invaded superior sagittal sinus in 3 patients compared to 2D TOF MRV, which revealed no flow signal (Figure 3).

The remaining 31 patients examined were found to be healthy with normal venous anatomy. The visibility of their 15 predefined venous structures that were

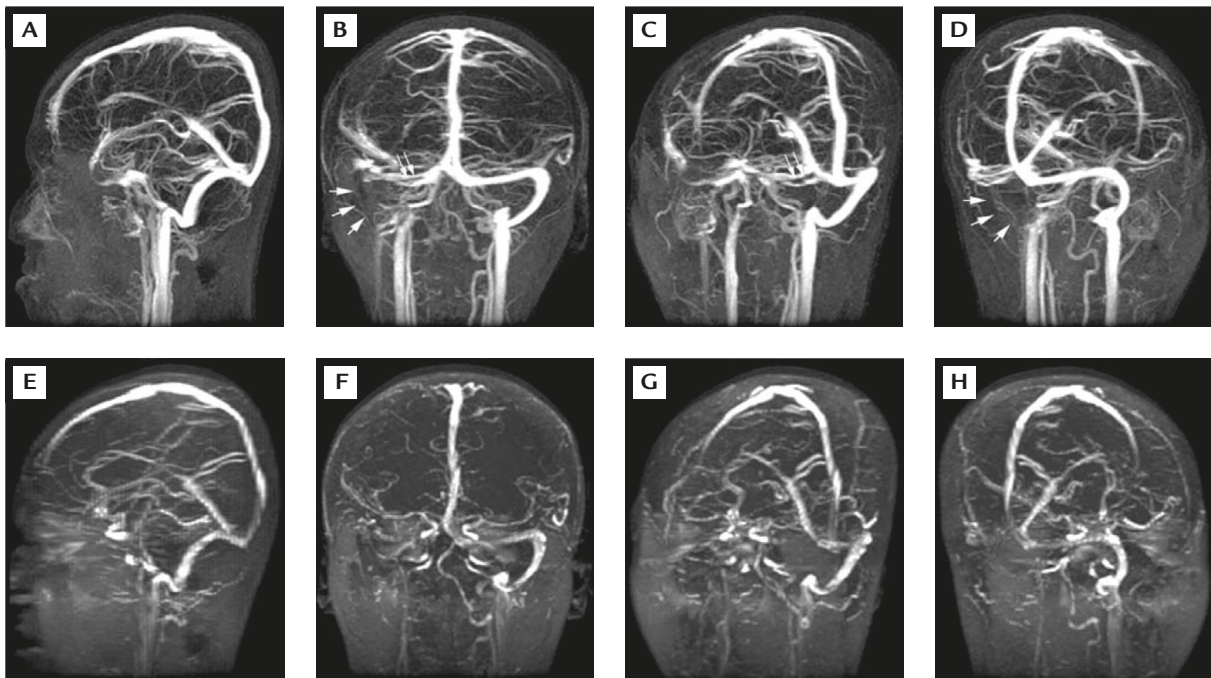


Figure 1. A patient with acute dural sinus thrombosis visualized using: (A–D) 3D GEC MRV; and (E–H) 2D TOF MRV. (A, E) Lateral maximum intensity projection. (B, F) Anteroposterior projection. (C, G) Left anterior oblique projection. (D, H) Right anterior oblique projection. 3D GEC MRV shows occlusion of the right sigmoid sinus [arrows in (B) and (D)] and acute thrombus as a filling defect in the right transverse sinus [double arrows in (B) and (C)]. Patency of the right internal jugular vein is noted via collateral reconstitution using 3D GEC MRV. 2D TOF MRV suggests ipsilateral dural sinus hypoplasia because of total nonvisualization of the right transverse and sigmoid sinuses, as well as the internal jugular vein (E–H).

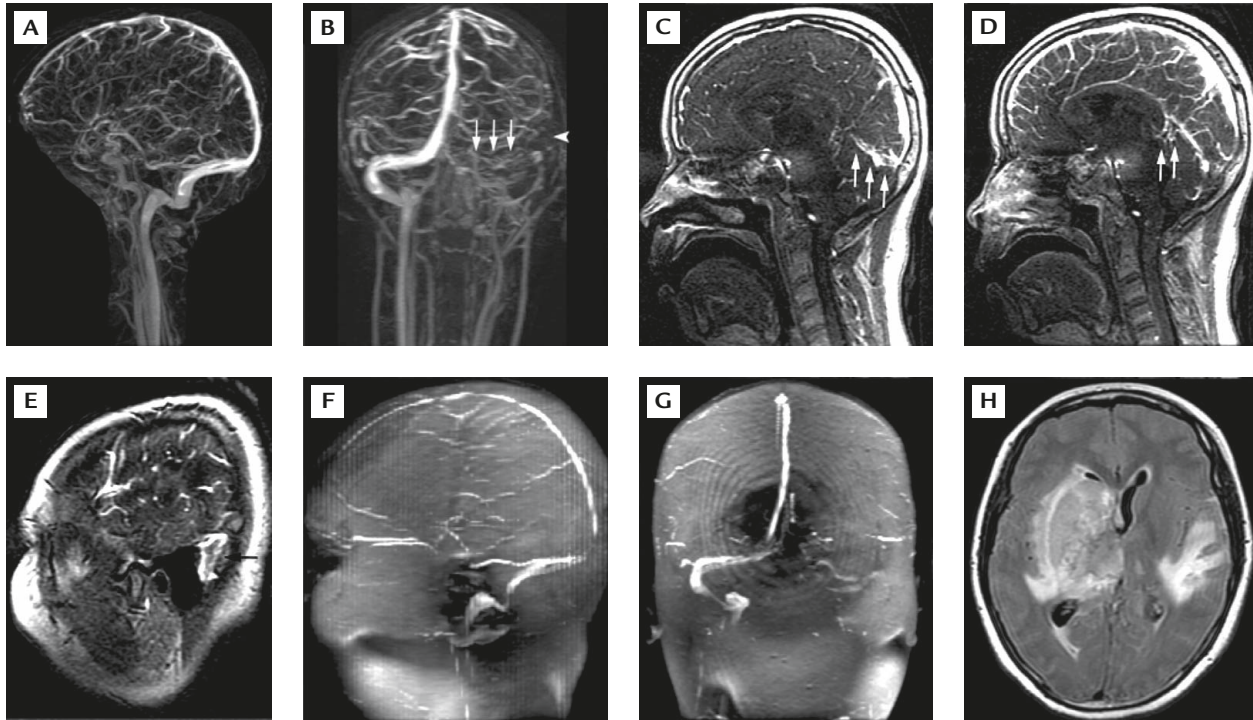


Figure 2. A patient with cerebral venous sinus thrombosis. (A) Lateral and (B) anteroposterior maximum-intensity projections of 3D GEC MRV show an absence of the straight sinus, the vein of Galen and internal cerebral veins (A), absent left transverse and sigmoid sinuses [arrows in (B)], and absent left vein of Labbe [arrowhead in (B)]. (C–E) Source images of 3D GEC MRV confirm hypointense clots in the straight sinus, vein of Galen and left sigmoid sinus (arrows). (F, G) Lateral and anteroposterior maximum-intensity projections of 2D TOF MRV show similar findings in the large venous sinuses, but the extent of thrombosis was overestimated with nonvisualization of the torcular herophili and inferior sagittal sinus, which indeed was due to pitfalls of 2D TOF MRV. (H) Axial fluid-attenuated inversion recovery MR imaging reveals heterogeneous hyperintense areas in the right basal ganglion, right thalamus and left temporal lobe, indicating venous infarction.

analyzed by the 2 independent readers is summarized in Table 1. The large dural venous structures (superior sagittal sinus, straight sinus, torcular herophili, right and left transverse sinuses, transverse-sigmoid junctions and sigmoid sinuses) were 100% (558 of 558 readings) completely visible using 3D GEC MRV, but only 64% (357 of 558 readings) completely visible using 2D TOF MRV. The torcular herophili ranked last, with only 14.5% (9 of 62 readings) complete visibility using 2D TOF MRV. The rate of complete visibility of the 15 predefined venous structures was 95.8% (891 of 930 readings) using 3D GEC MRV and only 62.1% (577 of 930) using 2D TOF MRV (Table 1, Figure 4). When the analysis of the 2 independent readers were compared, it was found that they agreed more often when using the 3D GEC MRV reading ($\kappa=0.93$) as opposed to the 2D TOF MRV reading ($\kappa=0.68$), indicating superior interobserver reliability with the 3D GEC MRV method.

Regarding the 22 patients diagnosed with either venous sinus thrombosis or tumor mentioned above, the sensitivity, specificity, positive predictive value, negative predictive value, and AUC for 2D TOF MRV

and 3D GEC MRV, including 95% confidence intervals, are given in Table 2. The AUC for 2D TOF MRV was 0.53 and for 3D GEC MRV was 0.91, indicating a significant difference between the 2 ($p<0.001$), with superiority of 3D GEC MRV over 2D TOF MRV (Figure 5).

Discussion

The use of 3D GEC MRV for imaging of the intracranial venous system has not been extensively studied.^{6,7} In Farb et al's initial experience with 3D GEC MRV,⁶ the region of interest of the 2D bolus-detection sequence was positioned at the cavernous carotid arteries. After the arrival of contrast material at the cavernous carotid level and an additional preprogrammed delay of 8 seconds, the 3D MR angiographic sequence was initiated. The delay of 8 seconds was chosen empirically on the basis of the mean normal cerebrovascular arterial-to-venous transit time. In the present study, we used a convenient and robust real-time fluoroscopic triggering method, by which the 3D MR angiographic

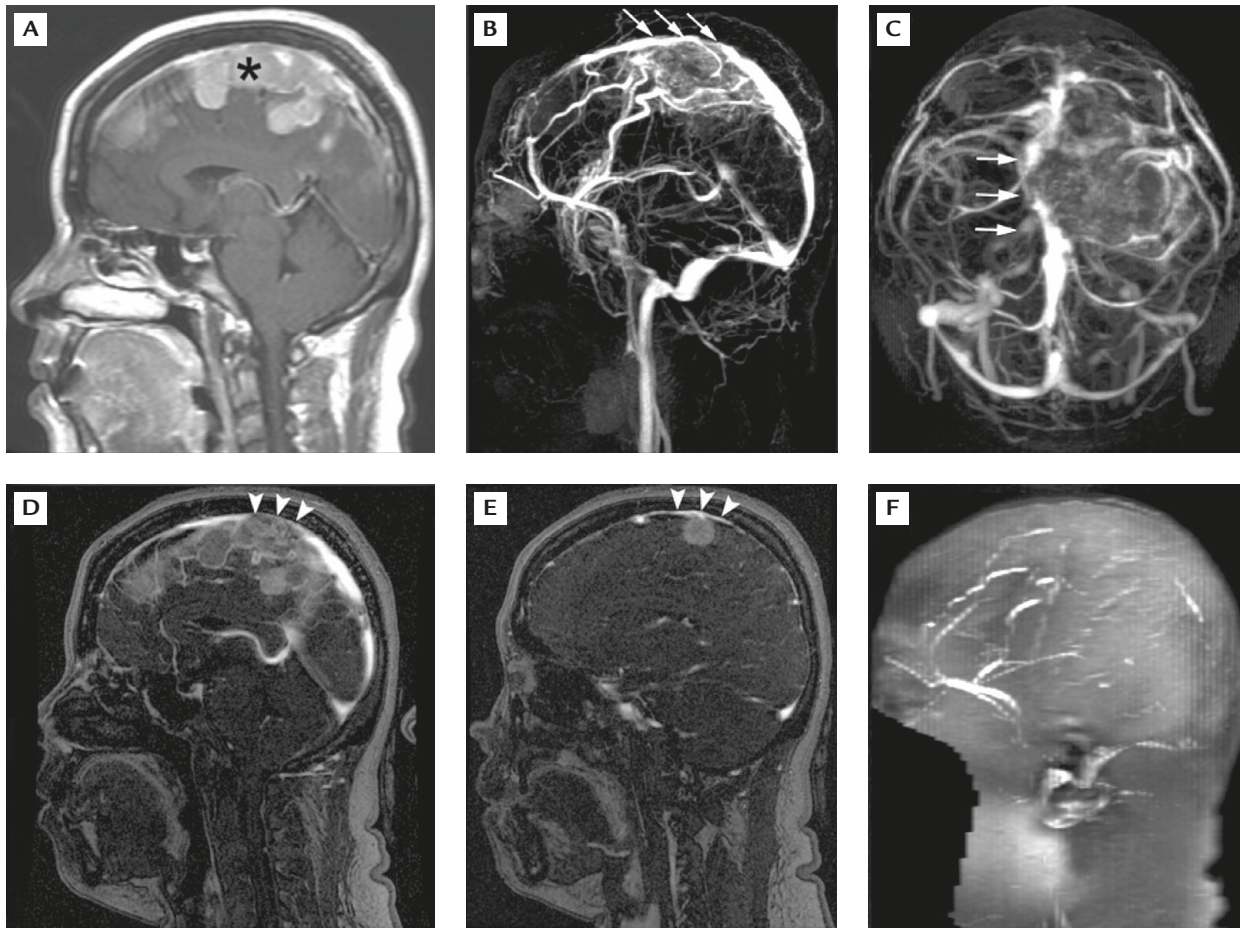


Figure 3. A patient with parasagittal meningioma. (A) Midline sagittal contrast-enhanced T1-weighted MR image reveals an enhanced tumor (asterisk). (B, C) Lateral and inferosuperior maximum intensity projections of 3D GEC MRV show infiltration of the tumor into the superior sagittal sinus (arrows). (D, E) Sagittal source images of 3D GEC MRV confirm the patency of the superior sagittal sinus with residual blood flow (arrowheads). (F) 2D TOF MRV lateral maximum intensity projection shows no flow signal in the invaded segment of the superior sagittal sinus.

sequence was initiated precisely when contrast medium was filling in the superior sagittal sinus, and the error of estimation of cerebrovascular arterial-to-venous transit time could be avoided.

The view order for this 3D GEC MRV angiographic sequence is an elliptic centric order phase encoding, similar to that previously reported.^{6-8,10} The elliptic centric ordering of phase encoding ensures that low-frequency k-space data (which dictate major structure signal intensity in the final image) are collected early in imaging, thus enhancing vessel contrast.

The advantage of superior venous structure depiction of 3D GEC MRV over 2D TOF MRV is important. When a venous structure is not seen, it is either hypoplastic or truly pathologically invaded or thrombosed. Our study demonstrated that 3D GEC MRV (95.8%) was better than 2D TOF MRV (62.1%) in the rate of complete visibility of the 15 predefined normal venous structures. 3D GEC MRV ($\kappa=0.93$)

also had superior interobserver reliability compared with 2D TOF MRV ($\kappa=0.68$). In addition, 2D TOF MRV often overestimated the extent of venous sinus thrombosis and tumoral sinus invasion because of misinterpretation of invisible venous structures as being pathologically thrombosed or invaded, which actually were patent but invisible due to artifactual signal loss or slower blood flow.

In cases of dural venous sinus thrombosis, other than the extent of thrombosis of the dural sinuses, we also want to know if there is any deep vein or cortical vein involvement, which is important in prediction of prognosis. The excellent quality and thin slices of source images of 3D GEC MRV allow us to achieve this goal, and it can be confidently used as a diagnostic tool in these conditions.⁷ The information provided can, as illustrated in Figures 1, 2 and 4, be used for the differential diagnosis of venous sinus thrombosis or slow flow/in-plane flow. In these cases, 2D TOF MRV was

Table 1. Results of 3D GEC MRV and 2D TOF MRV in 31 healthy patients*†

| Venous structure | 3D GEC | | | 2D TOF | | |
|-----------------------------|-------------|-------------------|--------------------|-------------|-------------------|--------------------|
| | Not visible | Partially visible | Completely visible | Not visible | Partially visible | Completely visible |
| Superior sagittal sinus | 0 | 0 | 62 | 0 | 9 | 53 |
| Inferior sagittal sinus | 0 | 10 | 52 | 22 | 17 | 23 |
| Torcular herophili | 0 | 0 | 62 | 4 | 49 | 9 |
| Straight sinus | 0 | 0 | 62 | 1 | 2 | 59 |
| Transverse sinus | | | | | | |
| Right | 0 | 0 | 62 | 1 | 15 | 46 |
| Left | 0 | 0 | 62 | 4 | 34 | 24 |
| Transverse-sigmoid junction | | | | | | |
| Right | 0 | 0 | 62 | 1 | 9 | 52 |
| Left | 0 | 0 | 62 | 4 | 15 | 43 |
| Sigmoid sinus | | | | | | |
| Right | 0 | 0 | 62 | 2 | 20 | 40 |
| Left | 0 | 0 | 62 | 18 | 13 | 31 |
| Internal cerebral vein | | | | | | |
| Right | 0 | 0 | 62 | 4 | 10 | 48 |
| Left | 0 | 2 | 60 | 2 | 17 | 43 |
| Basal vein of Rosenthal | | | | | | |
| Right | 3 | 7 | 52 | 26 | 11 | 25 |
| Left | 5 | 12 | 45 | 29 | 9 | 24 |
| Vein of Galen | 0 | 0 | 62 | 4 | 1 | 57 |
| Total | 8 (0.9) | 31 (3.3) | 891 (95.8) | 122 (13.1) | 231 (24.8) | 577 (62.1) |

*Data are presented as n or n (%); †results are for 31 patients from 2 independent readers for a total of 62 readings per structure (930 readings overall).

misleading and might result in an erroneous diagnosis. 3D GEC MRV may lead to false-negative results in patients with late-stage venous sinus thrombosis, as a chronic and/or partially recanalized thrombus may enhance mimicking blood flow.⁷ Therefore, a careful evaluation of source image data is needed.

In tumoral cases, especially in parasagittal meningiomas, total resection of the tumor may require removal of a portion of the superior sagittal sinus. In the case of a completely occluded sinus by tumor invasion, sufficient collaterals may have formed to allow total removal of the sinus. However, tumor resection may lead to abrupt venous infarction if the superior sagittal sinus is invaded but patent, which could not be well differentiated using 2D TOF MRV. In contrast, 3D GEC MRV clearly depicts residual blood flow in the invaded sinus and collateral cortical veins, which facilitates surgical planning. Our results agree with those of previous studies.^{11,12} Overall, the sensitivity/specificity of 3D GEC MRV were 90.9%/96.8%,

compared to 63.6%/48.4% for 2D TOF MRV. The present study indicates that 3D GEC MRV is useful for imaging of the intracranial venous system.

Our study has several limitations. First, conventional catheter angiography as gold standard was not available in the majority of cases due to its invasiveness and its potential risks; it was thus only reserved for those in whom MRV was non-conclusive. Second, the study design was retrospective and not randomized. We performed MRV only under clinical request to evaluate the intracranial venous system. Third, correlation with surgical findings was not available in tumoral cases, which was also attributed to the retrospective study design.

In conclusion, 3D GEC MRV is superior to 2D TOF MRV for providing more detail and high-quality images of the intracranial venous system. It is also our recommended method of choice for the diagnosis of dural venous sinus thrombosis as well as tumor invasion into dural sinuses.

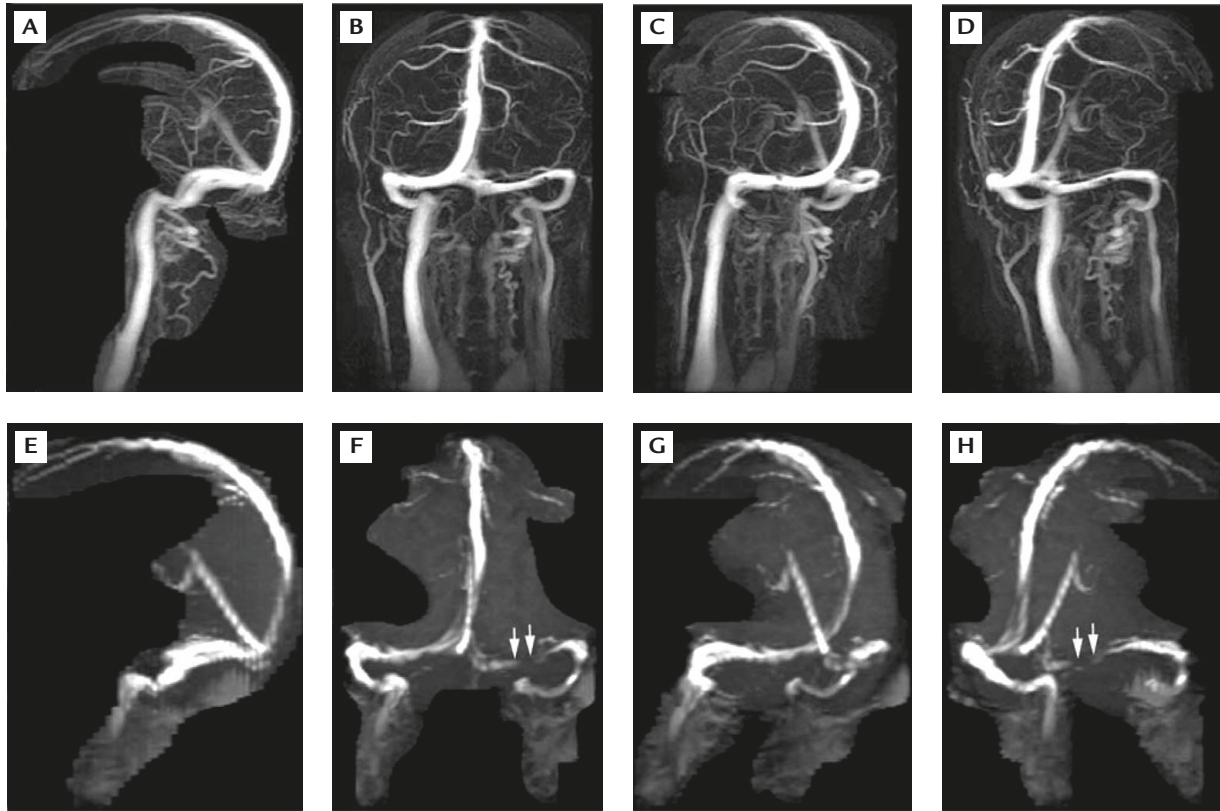


Figure 4. Venous anatomy of a healthy patient seen on: (A–D) 3D GEC MRV; and (E–H) 2D TOF MRV. (A, E) Lateral maximum intensity projection. (B, F) Anteroposterior projection. (C, G) Left anterior oblique projection. (D, H) Right anterior oblique projection. (B, D) 3D GEC MRV shows that the left transverse sinus is patent; (F, H) while narrowing is noted on 2D TOF MRV (arrows). This pitfall with the 2D TOF method was due to in-place flow. Note that the signal intensity and visibility of the cerebral veins and sinuses are superior when imaged with 3D GEC MRV than with 2D TOF MRV.

Table 2. Overall sensitivity, specificity, PPV, NPV and AUC of 3D GEC and 2D TOF MRV used to diagnose the 22 patients with venous sinus thrombosis and tumor (95% confidence intervals in parentheses)

| | Sensitivity (%) | Specificity (%) | PPV (%) | NPV (%) | AUC* |
|------------|------------------|------------------|------------------|-------------------|------------------|
| 3D GEC MRV | 90.9 (61.5–99.2) | 96.8 (72.5–99.9) | 95.2 (68.7–99.9) | 93.8 (64.37–99.8) | 0.91 (0.78–1.00) |
| 2D TOF MRV | 63.6 (34.9–90.1) | 48.4 (22.5–75.4) | 46.7 (20.2–73.8) | 65.2 (36.7–92.4) | 0.53 (0.32–0.75) |

* $p < 0.001$. PPV = positive predictive value; NPV = negative predictive value; AUC = area under the receiver operating characteristic curve.

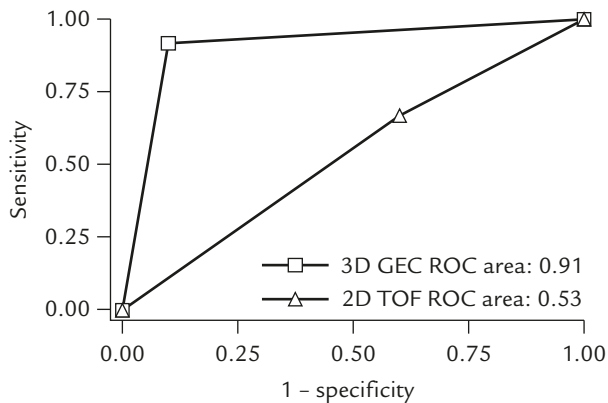


Figure 5. Areas under the receiver operating characteristic (ROC) curves of 2D TOF MRV and 3D GEC MRV.

Acknowledgments

This work was supported in part by grants from the National Science Council (NSC 97-2314-B-075B-010-MY3) and Kaohsiung Veterans General Hospital (VGHKS96-61, VGHKS98-68).

References

1. Yasargil MG, Damur M. Thrombosis of the cerebral veins dural sinuses. In: Newton TH, Potts DG, eds. *Radiology of the Skull and Brain: Angiography*. St. Louis: Mosby-Year Book, 1974: 2375–400.
2. Willinsky RA, Taylor SM, terBrugge K, Farb RI, Tomlinson G, Montanera W. Neurologic complications of

- cerebral angiography: prospective analysis of 2,899 procedures and review of the literature. *Radiology* 2003;227:522–8.
3. Kirchhof K, Welzel T, Jansen O, Sartor K. More reliable non-invasive visualization of the cerebral veins and dural sinuses: comparison of three MR angiographic techniques. *Radiology* 2002;224:804–10.
 4. Liauw L, van Buchem MA, Spilt A, de Bruïne FT, van den Berg R, Hermans J, Wasser MN. MR angiography of the intracranial venous system. *Radiology* 2000;214:678–82.
 5. Ayanzen RH, Bird CR, Keller PJ, McCully FJ, Theobald MR, Heiserman JE. Cerebral MR venography: normal anatomy and potential diagnostic pitfalls. *AJNR Am J Neuroradiol* 2000;21:74–8.
 6. Farb RI, Scott JN, Willinsky RA, Montanera WJ, Wright GA, terBrugge KG. Intracranial venous system: gadolinium-enhanced three-dimensional MR venography with auto-triggered elliptic centric-ordered sequence—initial experience. *Radiology* 2003;226:203–9.
 7. Klingebiel R, Bauknecht HC, Bohner G, Kirsch R, Berger J, Masuhr F. Comparative evaluation of 2D time-of-flight and 3D elliptic centric contrast-enhanced MR venography in patients with presumptive cerebral venous and sinus thrombosis. *Eur J Neurol* 2007;14:139–43.
 8. Wilman AH, Riederer SJ, King BF, Debbins JP, Rossman PJ, Ehman RL. Fluoroscopically triggered contrast-enhanced three-dimensional MR angiography with elliptical centric view order: application to the renal arteries. *Radiology* 1997;205:137–46.
 9. Park SH, Goo JM, Jo CH. Receiver operating characteristic (ROC) curve: practical review for radiologists. *Korean J Radiol* 2004;5:11–8.
 10. Huston J III, Fain SB, Wald JT, Luetmer PH, Rydberg CH, Covarrubias DJ, Riederer SJ, et al. Carotid artery: elliptic centric contrast-enhanced MR angiography compared with conventional angiography. *Radiology* 2001;218:138–43.
 11. Bozzao A, Finocchi V, Romano A, Ferrante M, Fasoli F, Trillò G, Ferrante L, et al. Role of contrast-enhanced MR venography in the preoperative evaluation of parasagittal meningiomas. *Eur Radiol* 2005;15:1790–6.
 12. Lee JM, Jung S, Moon KS, Seo JJ, Kim IY, Jung TY, Lee JK, et al. Preoperative evaluation of venous systems with 3-dimensional contrast-enhanced magnetic resonance venography in brain tumors: comparison with time-of-flight magnetic resonance venography and digital subtraction angiography. *Surg Neurol* 2005;64:128–34.